Top Catal (2012) 55:209–217
DOI 10.1007/s11244-012-9789-z

ORIGINAL PAPER

Bench- and Pilot-Scale Studies of Reaction and Regeneration of Ni–Mg–K/Al_2O_3 for Catalytic Conditioning of Biomass-Derived Syngas

Kimberly A. Magrini-Bair · Whitney S. Jablonski · Yves O. Parent · Matthew M. Yung

Published online: 7 April 2012

Abstract The National Renewable Energy Laboratory (NREL) is collaborating with both industrial and academic partners to develop technologies to help enable commercialization of biofuels produced from lignocellulosic biomass feedstocks. The focus of this paper is to report how various operating processes, utilized in-house and by collaborators, influence the catalytic activity during conditioning of biomass-derived syngas. Efficient cleaning and conditioning of biomass-derived syngas for use in fuel synthesis continues to be a significant technical barrier to commercialization. Multifunctional, fluidizable catalysts are being developed to reform undesired tars and light hydrocarbons, especially methane, to additional syngas, which can improve utilization of biomass carbon. This approach also eliminates both the need for downstream methane reforming and the production of an aqueous waste stream from tar scrubbing. This work was conducted with NiMgK/Al_2O_3 catalysts. These catalysts were assessed for methane reforming performance in (i) fixed-bed, bench-scale tests with model syngas simulating that produced by oak gasification, and in pilot-scale, (ii) fluidized tests with actual oak-derived syngas, and (iii) recirculating/regenerating tests using model syngas. Bench-scale tests showed that the catalyst could be completely regenerated over several reforming reaction cycles. Pilot-scale tests using raw syngas showed that the catalyst lost activity from cycle to cycle when it was regenerated, though it was shown that bench-scale regeneration by steam oxidation and H_2 reduction did not cause this deactivation. Characterization by TPR indicates that the loss of a low temperature nickel oxide reduction feature is related to the catalyst deactivation, which is ascribed to nickel being incorporated into a spinel nickel aluminate that is not reduced with the given activation protocol. Results for 100 h time-on-stream using a recirculating/regenerating reactor suggest that this type of process could be employed to keep a high level of steady-state reforming activity, without permanent deactivation of the catalyst. Additionally, the differences in catalyst performance using a simulated and real, biomass-derived syngas stream indicate that there are components present in the real stream that are not adequately modeled in the syngas stream. Heavy tars and polycyclic aromatics are known to be present in real syngas, and the use of benzene and naphthalene as surrogates may be insufficient. In addition, some inorganics found in biomass, which become concentrated in the ash following biomass gasification, may be transported to the reforming reactor where they can interact with catalysts. Therefore, in order to gain more representative results for how a catalyst would perform on an industrially-relevant scale, with real contaminants, appropriate small-scale biomass solids feeders or slipstreams of real process gas should be employed.

Keywords Reforming · Biomass · Syngas · Ni catalyst · Deactivation · Regeneration

Special issue of Biomass Conversion Papers from 2011 AIChE Conference.

K. A. Magrini-Bair (✉) · W. S. Jablonski · M. M. Yung
National Bioenergy Center, National Renewable Energy Laboratory, 1617 Cole Blvd., Golden, CO 80401, USA
e-mail: Kim.Magrini@nrel.gov

Y. O. Parent
Chemical Engineering Consulting Services LLC,
3925 Douglas Mountain Drive, Golden, CO 80403-7701, USA

1 Introduction

Thermochemical conversion of biomass to syngas, via gasification, is one of the routes that can be used to create

fuels and chemical products. In this process, the raw, biomass-derived syngas contains the building blocks of carbon monoxide and hydrogen as well as undesired species (e.g., tars, hydrocarbons, methane, hydrogen sulfide, ammonia, hydrogen chloride, and other trace contaminants) [1, 2]. These undesired species must be removed before syngas can be efficiently used for synthesis of liquid fuels such as mixed alcohols and Fischer–Tropsch products. Tar formation during biomass gasification is one of the primary challenges preventing commercialization of this technology, due to several process issues, such as catalyst coking, and condensation on downstream equipment. Though the definition of tars varies, they generally comprise the condensable fraction of organic gasification products, mostly aromatic compounds larger than benzene such as toluene and naphthalene [1–4]. Tars can be removed by wet scrubbing or catalytic conditioning, which can cost as much as the combined total of the other process costs to produce ethanol [5, 6]. Although gas cleanup can constitute a significant portion of the process cost, catalytic conditioning can significantly improve the carbon utilization of biomass by reforming hydrocarbons into additional syngas. There are several reviews describing catalysts used in a fixed-bed configuration for syngas tar reforming using nickel on alumina and ceramic supports [2, 4], and on olivine, dolomites, and perovskites [7–10]. Other excellent reviews provide additional insight into the work that has been done on catalytic conditioning of biomass-derived syngas [11, 12].

Numerous methods have been used for incorporating catalytic tar destruction into biomass gasification systems including (1) catalysts within the gasifier as the fluidizing media [13, 14], (2) steam reforming catalysts in a downstream, fixed-bed reactor [15], (3) downstream fluidized bed systems [16, 17], and (4) downstream monolithic catalysts [18]. All of these processes can be significantly slowed by rapid catalyst deactivation from coke formation and sulfur exposure, especially in fixed-bed systems [19], while the use of fluidized catalyst beds can significantly reduce the impact of these processes [14, 19, 20].

The primary limitation of hot gas catalytic tar cracking is catalyst deactivation [1, 5], which occurs from both physical and chemical processes associated with the harsh reaction conditions and impurities in the biomass-derived feed stream. Attrition, coking, sintering, phase changes, and sulfur poisoning are the primary deactivation mechanisms that can affect the efficient catalytic conditioning of biomass-derived syngas, though the cumulative effects of the other trace inorganic species that are present in biomass (e.g., Si, Al, Ti, Fe, Ca, Mg, Na, K, P, S, and Cl) must also be considered [21]. The deactivation of Ni catalysts by sulfur poisoning has been studied by many investigators and has been attributed to the formation of nickel sulfides (Ni_xS_y) [22–24]. Both this work on Ni/Al_2O_3-type catalysts exposed to H_2S and that of other authors indicate that a nickel sulfide (or, in general, a metal sulfide) can be regenerated with steam to form H_2S and a metal oxide [25–28] followed by reduction in H_2 to recover the reduced metal as shown in Eqs. 1, 2, and 3.

$$Ni + H_2S \leftrightarrow Ni - S + H_2 \quad (1)$$

$$Ni - S + H_2O \leftrightarrow NiO + H_2S \quad (2)$$

$$NiO + H_2 \leftrightarrow Ni + H_2O \quad (3)$$

While reports of regenerating tar cracking catalysts used with raw biomass-derived syngas are few, several recent articles describe fixed-bed processes focused on recovering catalyst activity after deactivation using model syngas containing hydrogen sulfide. Ashrafi et al. [23] identified two viable methods for reactivating nickel based catalysts used to reform methane in model syngas containing up to 145 ppm hydrogen sulfide (H_2S): (1) sulfur removal from the feed gas, which resulted in nearly complete regeneration though the time to regain activity was significantly longer than actual reforming time on stream; and (2) raising reforming temperatures to >900 °C achieved 85 % methane conversion compared to 30 % at 800 °C. They also found that oxidative treatment formed less active nickel aluminate with incomplete recovery of activity. Other work has shown that oxidative treatment restores most though not all reforming activity after exposure to sulfur [27] with nickel surface restructuring likely causing incomplete regeneration as nickel sulfur melts (alloys) have been found on catalysts used for hot syngas cleaning [24].

The surface nickel sulfur species that form are likely related to reactor configuration, syngas composition, and reaction temperature and may require specific regeneration processes to regain catalyst activity. Hepola [22] found that sulfur adsorption on nickel surfaces is strongly impacted by temperature: at >900 °C, sulfur irreversibly adsorbed as a monolayer while at <900 °C, multi-layer polysulfide's formed which were reversibly desorbed in hydrogen until only a monolayer remained on the surface. Rostrup Nielsen [28] successfully used steam regeneration at 700 °C to remove 80 % of adsorbed sulfur on both promoted and unpromoted nickel reforming catalysts with the remaining sulfur species undetermined. EXAFS studies of deactivated and steam and air regenerated nickel reforming catalysts used with oak-derived syngas showed that residual sulfur remained on the surface after regeneration and also revealed the formation of a Ni, Mg spinel that is likely less active than nickel for subsequent reforming [29]. Others have identified nickel oxide formation via XPS after oxidative treatment of nickel catalysts used with cedar-derived syngas [30]. Rostrup-Nielsen [31] used high temperatures

and pressures of steam and hydrogen to regenerate nickel based catalysts, which is similar to the process we have employed, which includes sequential steam and hydrogen exposure at ambient pressure and process conditions. Taken together, these regeneration results generally show that most hydrogen sulfide can be removed from supported nickel surfaces, though the extent of removal and subsequent activity recovery are highly dependent on the composition of adsorbed nickel sulfur species, feed gas composition, catalyst contact time, reaction temperature, and regeneration gas composition. Thus, efficient regeneration processes need to be developed considering specific process conditions.

2 Experimental

2.1 Catalyst Synthesis

The attrition-resistant catalyst used in this work was prepared via incipient-wetness impregnation onto an alpha-alumina-type support (AD90) provided by CoorsTek Ceramics. The AD90 support is 90 % alpha alumina in a particle size range of 100–250 μm and was used to prepare several 75 kg batches of Ni-based catalyst. Catalyst composition, modeled on commercial naphtha reforming catalysts, contained 2.4 wt% Mg, 6.1 wt% Ni, and 3.9 wt% K. An aqueous solution of nickel (Ni), potassium (K), and magnesium (Mg) nitrate salts (99 % Ni $(NO_3)_2{\cdot}6H_2O$, Mg $(NO_3)_2{\cdot}6H_2O$ (Alfa Aesar), and 99 % KNO_3 (Aldrich) was used for the impregnation. The wet solids were dried at 100 °C and then calcined at 650 °C in air in a rotary calciner to decompose the metal salts into the corresponding metal oxides. MgO and K_2O remain as oxides on the surface. Nickel oxides are reduced to catalytic metal species on the support surface in hydrogen at 850 °C in a separate step prior to reforming. The results from the bench-scale experiments and pilot-scale experiments using real syngas were done on this catalyst, $NiMgK/Al_2O_3$. An additional catalyst batch was synthesized which contained less potassium, nominally consisting of 2.4 wt% Mg, 6.1 wt% Ni, and 0.39 % K, but was otherwise synthesized in the same manner. This catalyst, $NiMgK_{0.1}/Al_2O_3$, was used in the recirculating/regenerating reactor tests. ICP was conducted with a Spectro Instruments Arcos spectrometer, and these results are shown in Table 1.

2.2 Pilot- and Bench-Scale Syngas Compositions

The representative syngas composition produced from indirect oak gasification is shown in Table 2. From this, a model syngas composition (Table 2) was derived for use in the bench-scale experiments. Olefins, paraffins, and acetylene were simulated using ethylene and all poly-cyclic aromatic hydrocarbons (tars) and benzene were simulated using benzene.

Table 1 ICP compositional analysis of Ni, Mg, and K content of freshly synthesized catalysts

Catalyst	Ni (wt%)	Mg (wt%)	K (wt%)
$NiMgK/Al_2O_3$	6.1	2.4	4.0
$NiMgK_{0.1}/Al_2O_3$	6.0	2.3	0.43

Table 2 Oak-derived and model syngas compositions used in pilot and bench-scale reforming catalyst evaluation (dry basis)

Species	Raw syngas Volume %	Model syngas Volume %
H_2	27.13	30
CH_4	14.6	15
CO	33.65	30
CO_2	18.36	18.5
C_2H_2	0.49	–
C_2H_4	4.62	6.42
C_3H_6	0.12	–
C_3H_8	0.95	–
1-C_4H_4	0.07	–
Benzene	0.004	0.075
Total tars[a]	26,500 mg/Nm^3	–
Total	100	100

[a] Total tars are masses >78 amu and comprise toluene, phenol, cresol, naphthalene, anthracene, and phenanthrene

2.3 Reforming Reaction Studies

An in-house constructed, fixed-bed reactor system was used to conduct reforming reactions using model syngas. The reaction system, described in detail elsewhere [15], utilized multiple mass flow controllers to generate a model syngas composition similar to that obtained from oak-gasification (as shown in Table 2). A peristaltic pump was used to introduce water to an ultrasonic nozzle placed above a quartz wool plug located above the catalyst bed, which enabled a fine mist of water vapor to be fed to the reactor, allowing for rapid volatilization. Process data were recorded by an OPTO 22 data acquisition system. The reactor product gas was sent to a condenser to remove excess steam and was then further dried using a Nafion membrane dryer with countercurrent nitrogen sweep gas. On-line process gas analysis provided comprehensive reaction gas composition. Product gas was sampled every 4 min by an on-line Varian Micro gas chromatograph that quantified helium (used as tracer gas), hydrogen, oxygen, nitrogen, methane, CO, CO_2, ethylene, ethane, benzene,

Table 3 Experimental conditions during bench-scale reforming reaction including steam regeneration and H_2 reduction steps (wet basis)

	Reforming	Regeneration	Reduction
Helium, mol%	2.8	5	
Hydrogen, mol%			28
Nitrogen, mol%	5.4	32.6	72
Syngas[a], mol%	29.4		
Steam, mol%	62.4	62.4	
H_2S, ppm	20		
Total, mol%	100	100	100
S/C	7.5	n/a	n/a
GHSV, h^{-1}	119,400	114,300	114,300
Temperature, °C	900	850	850
Time, min	30	60	300

n/a not available

[a] Syngas composition shown in Table 2

and acetylene. Carbon balances were calculated based on the flow rates and concentration of the gas components, and ranged from 99 to 101 % for all experiments.

When multiple reaction cycles were conducted at the bench-scale, the process parameters, including regeneration conditions, are shown in Table 3. Additional details on the pilot-plant reaction studies have been previously reported [29]. Model syngas reforming using a separate 75 kg batch of NREL catalyst of the same composition was also tested by an industrial collaborator using a pilot-scale recirculating/regenerating system that had H_2S spiked in at intervals to evaluate impact on reforming catalyst activity. Methane conversion was used to track catalyst performance at temperatures from 880 to 925 °C, 80 or 160 ppmv H_2S, and a surrogate tar loading of 32,000 mg per normal cubic meter.

2.4 Catalyst Characterization

Fresh and spent catalyst samples were analyzed via H_2 temperature-programmed reduction (TPR), X-ray diffraction (XRD), inductively-coupled plasma spectroscopy (ICP), and scanning electron microscopy with energy dispersive spectroscopy (SEM/EDS). TPR analysis was conducted with an Altamira Instruments AMI-390 temperature programmed reaction system equipped with thermal conductivity detectors. Quartz U-tube reactors were loaded with 100 mg of catalyst, which was held in place between two quartz wool plugs. Samples underwent a treatment in helium at 300 °C prior to TPR steps consisting of heating from 50 to 850 °C in 10 % H_2/Ar at 10 °C/min with a 30 min hold at maximum temperature. Post-reaction catalysts were oxidized at 850 °C in 10 % O_2/Ar prior to obtaining TPR profiles. XRD was conducted on a Scintag XGEN 4000 spectrometer equipped with a CuKα X-ray source, using a 0.03° step size, in order to determine the crystalline structures of the catalysts. SEM/EDS was conducted on uncoated, post-reaction catalysts using an EVEX Mini-SEM with an accelerating voltage of either 5 or 15 keV.

3 Results and Discussion

3.1 Pilot and Bench-Scale Reaction Results

Reaction tests using a fluidized bed, pilot-scale reactor with 60 kg of the fluidizable Ni–Mg–K/Al_2O_3 NREL catalyst were conducted for ten cycles of steam reforming tars and hydrocarbons in oak-derived syngas. Between reaction cycles, the catalyst was regenerated using (i) steaming followed by (ii) H_2 reduction, as has been used industrially [25, 28], and these results have been previously reported [29]. Due to the nearly complete conversion of tars and other hydrocarbons during these runs, it was necessary to use the methane conversion to compare catalytic activity among reaction cycles. Figure 1 shows the initial methane conversion for each of the ten reaction cycles during this run, which constitute a total of ~22 h time-on-stream. Within each reaction cycle, there was a decrease in methane conversion that was mainly attributed to H_2S deactivation, while the clear decrease in activity over multiple

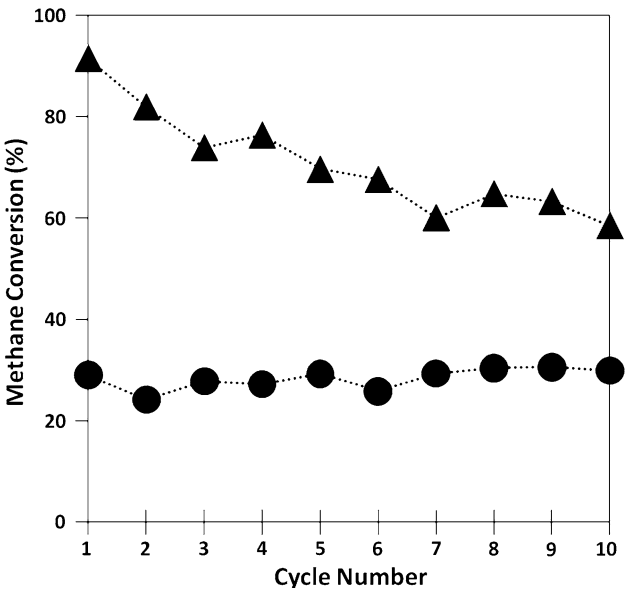

Fig. 1 Initial methane conversion on NREL NiMgK/Al_2O_3 catalyst during ten reaction cycles at 900 °C during (i) pilot-plant syngas conditioning of oak-derived syngas with 60 kg catalyst, 15 kg/h biomass, 15 kg/h H_2O (*filled triangle*), and (ii) bench-scale experiments with 100 mg catalyst, 200 sccm (dry), 15 % CH_4, balance He, 0.3 mL/min H_2O (*filled circle*)

reaction cycles has been primarily attributed to the loss of reducible nickel species by phase transformation into difficult-to-reduce, oxidized forms of nickel and nickel-sulfur species [29, 32]. These results and our previous work that demonstrated 240 h of continuous reforming of sulfur-free pyrolysis oils to produce syngas [16], suggest that it is the presence of H_2S, not tars that primarily cause catalyst deactivation during raw syngas processing.

To better understand the causes of deactivation during multiple cycles of pilot-scale conditioning of biomass-derived syngas, a bench-scale experiment was designed in order to test whether the oxidation and reduction cycling that occur during regeneration were contributing to catalyst deactivation from cycle to cycle. Conditions in this experiment were chosen to minimize any deactivation during the course of any single reaction cycle, in order to help isolate the effects of the regeneration procedures on activity. Ten cycles of steam methane reforming using a high steam-to-carbon ratio (S/C = 9) were conducted in the absence of H_2S, and the results are shown in Fig. 1. Within each reaction cycle, there was no deactivation of the catalyst and, over the course of the experiment, there was no significant change in the catalyst activity from first to the tenth reaction cycle. This indicates that the steam oxidation and H_2 reduction cycles, which the catalyst experiences during regeneration, have a negligible effect on catalyst deactivation. It should also be noted that the conversion values from the pilot and bench-scale experiments should not be directly compared with each other due to differences in reactor geometry, steam-to-carbon ratio, residence time, and gas phase composition. The methane conversion values in Fig. 1 should be compared only to the other cycles from the same experiment to assess changes in the catalyst activity from cycle to cycle.

3.2 Bench-Scale Experiments on Fresh and Spent Catalyst from the Pilot-Scale

In order to directly compare the fresh catalyst with the spent catalyst from the pilot-scale (following the tenth reaction cycle), both catalyst samples were tested for multiple conditioning cycles of a model syngas containing H_2S (as presented in Tables 2, 3). In these experiments, both catalysts were exposed to the same reaction and regeneration conditions with the exception that the spent catalyst from the pilot-scale was directly placed into the bench-scale reactor and no H_2 reduction was performed prior to beginning the first reaction cycle, in order to keep it in its deactivated state. The results from these experiments are shown in Fig. 2.

For the fresh catalyst, the introduction of H_2S leads to significant decrease in the methane conversion. However, when the catalyst is regenerated using steam oxidation and

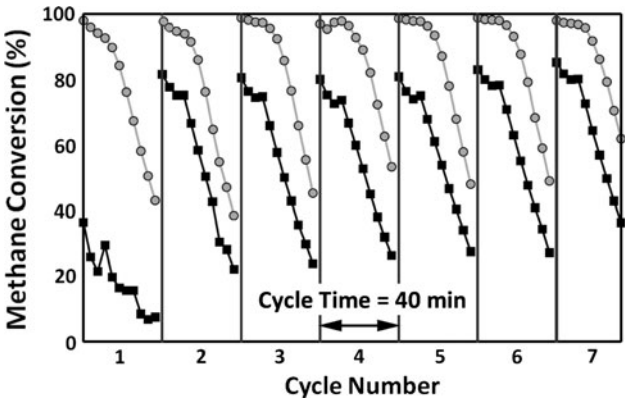

Fig. 2 Methane conversion during bench-scale conditioning of model biomass-derived syngas at 900 °C with a $NiMgK/Al_2O_3$ catalyst that was either (i) fresh (*filled circle*) or (ii) post-reaction from pilot-scale syngas conditioning studies (*filled square*). Tables 2, 3 contain reaction parameters for the processes, and H_2S was introduced at 10 min into each 40 min reaction cycle

H_2 reduction, the activity was completely recovered and there was no observable deactivation over seven reaction cycles. When the spent catalyst from the pilot-scale experiment was tested in the reactor, its activity during the first cycle was significantly lower than that of the fresh catalyst, which was to be expected since it was used in its deactivated state. When the pilot catalyst was regenerated, however, it regained a significant amount of activity, though its activity was still somewhat lower than that of the fresh catalyst. During the subsequent reaction cycles (2–7), the pilot catalyst was fully regenerated from cycle-to-cycle. This regeneration result was better than that achieved in the fluidized-bed reactor of the pilot-plant using real syngas. This difference between the effectiveness of regeneration between fixed-bed catalysts used with model syngas and fluidized-bed catalysts used with biomass-derived syngas is being explored and may be due to incomplete regeneration of surface nickel sites in the fluidized bed, incomplete removal of sulfur species, and possible buildup of other contaminants contained in the raw syngas (e.g., alkali, or Cl from HCl adsorption). In summary, these results indicate that during the pilot-plant conditioning studies, either (i) the regeneration protocol is insufficient to fully restore activity or (ii) there are other deactivation mechanisms that are not being captured during the bench-scale experiments which are leading to the loss of activity from cycle-to-cycle (e.g., attrition, poisoning by trace contaminants, and temperature incursions resulting in phase or structural changes).

3.3 Recirculating/Regenerating Pilot-Plant Tests

Ongoing, unpublished, work in our laboratory and with an industrial partner indicates that the extent of poisoning (i.e., length of contact time with H_2S) prior to regeneration

has some effect on the efficacy of regeneration. Namely, if a reforming catalyst is exposed to H_2S for a long period, its activity following regeneration will be less than if it had been exposed to H_2S for a shorter period and then underwent the same regeneration protocol. This finding would indicate that a recirculating/regenerating reactor, like those found in fluidized catalytic cracking (FCC) units to burn of coke and regenerate catalysts, could be suitable for use in catalytic-conditioning of biomass-derived syngas. In the recirculating/regenerating reactor, the exposure time to reaction gases can be on the order of seconds, and this allows the catalyst to maintain a high level of activity following regeneration.

An industrial collaborator, interested in using biomass-derived syngas to produce liquid biofuels, tested the NREL Ni–Mg–K/Al_2O_3 catalyst in a recirculating/regenerating reactor to condition model biomass-derived syngas at various temperatures, H_2S concentrations, and tar content. The model syngas composition was similar to that shown in Table 4 and the tar consisted of surrogate compounds such as benzene and naphthalene. While the complete details from these reaction tests are not available, the results shown in Table 4 for various operating conditions indicate that the Ni–Mg–K/Al_2O_3 catalyst is able to achieve a high steady-state conversion of methane, as well as other tars and hydrocarbons. This coupled recirculating/regenerating system offers the ability to limit sulfur buildup while regenerating deactivated catalyst in the same system. These results demonstrated that a recirculating/regenerating reactor could be employed to effectively catalytically condition biomass-derived syngas, and this process might be viable for demonstration or commercial scale use.

3.4 Characterization of Post-reaction Catalysts

Post-reaction analysis by TPR, XRD, and SEM/EDS was conducted on the catalysts used in (i) bench-scale reaction studies, (ii) pilot-scale studies in a fluidized bed reactor using raw biomass-derived syngas, and (iii) the recirculating/regenerating reactor at the pilot-scale with model syngas. The bench-scale catalysts were evaluated after each regeneration cycle to determine if differences in Ni species could be identified and correlated with reaction and regeneration conditions. Similar analyses were performed with regenerated pilot-scale catalyst after completion of each syngas conditioning cycle. Lastly, catalyst samples after 100 h of recirculating/regenerating reforming with model syngas were analyzed. The XRD profiles of the regenerated bench-scale catalysts were found to have minimal variation (data not shown) while significant differences were observed among the pilot-scale catalysts [29] in which spinel nickel aluminate formation increased with increasing raw syngas reforming cycles.

Table 4 Steady-state activity using a $NiMgK_{0.1}/Al_2O_3$ catalyst (75 kg) in a recirculating-regenerating, pilot-scale reactor for conditioning of model syngas containing surrogate tars (e.g., benzene, naphthalene), with >100 h time-on-stream

Run No	CH_4 Conv. (%)	Temp. (°C)	H_2S (ppm)	Tars (mg/Nm^3)
1	99.0	880	0	–
2	90.5	890	80	–
3	93.2	925	160	–
4	91.4	910	160	32,000

Figure 3a compares XRD profiles of post-reaction catalysts used for steam reforming of (i) model syngas in a bench-scale, fixed-bed reactor; (ii) real syngas in a pilot-plant, fluidized-bed reactor; and (iii) model syngas in a pilot-plant, recirculating/regenerating reactor. The post-reaction catalyst from the pilot-scale test with real syngas shows the highest $NiAl_2O_4$ content of the three samples. Metallic nickel and spinel nickel aluminate ($NiAl_2O_4$) can be seen in addition to peaks characteristic of the alumina support (AD90). The intensity of the spinel $NiAl_2O_4$ phase may be associated with loss of reforming activity and the amount of $NiAl_2O_4$ on the bench-scale sample is less than what has been observed on the same catalyst tested on the pilot-scale [29]. The nickel aluminate formation could be accelerated by temperature spikes or cumulative time spent at high temperatures [33], as well as a component in the raw syngas. The additional feature at 62.5° 2θ on catalyst (iii) is due to NiO, which was not present in the other samples. This shows that the catalyst collected from the recirculating/regenerating reactor contained a mixture of nickel phases (oxide and metallic) in addition to the spinel. The presence of the NiO phase also explains the decreased intensity of the NiO phase on the same sample, as the nickel is divided among these phases.

Figure 3b compares TPR profiles for the same samples described in Fig. 3a. There are two distinct features in the TPR profiles. The low temperature feature (~400 °C) is attributed to free nickel oxide (NiO) that weakly interacts with the support [15, 35]. The high temperature feature (850 °C) is attributed nickel strongly interacting with the support, possibly stabilized by Mg or in a spinel structure such as nickel aluminate ($NiAl_2O_4$) or a (Ni, Mg)Al_2O_4 solid solution [34]. For the catalyst used with real syngas, TPR shows that most of the nickel is strongly interacting with the support, showing only the high temperature reduction feature. In contrast, as compared to the catalyst used in real syngas, the catalysts used with model syngas (fixed-bed bench and recirculating/regenerating pilot-scale) had significantly more free nickel oxide as indicated by the larger reduction features at 400 °C. In comparing the TPR profiles with the reaction results, it appears that the loss of

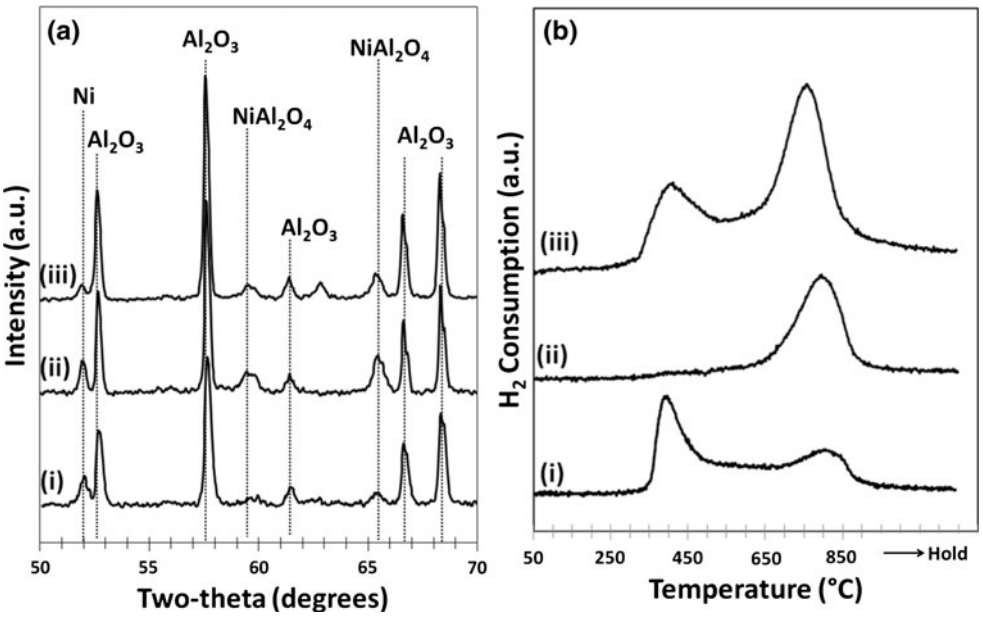

Fig. 3 **a** XRD patterns and **b** H_2 TPR profiles of post-reaction catalysts tested in (*i*) fixed-bed reactor, bench-scale conditions with model syngas ($NiMgK/Al_2O_3$), (*ii*) pilot-plant fluidized bed reactor with real syngas ($NiMgK/Al_2O_3$), and (*iii*) pilot-plant recirculating/regenerating reactor using model syngas ($NiMgK_{0.1}/Al_2O_3$)

the low temperature reduction feature, attributed to free NiO, coincides with decreased activity during multiple reforming cycles. The process that is responsible for the loss of the low temperature reduction feature is uncertain and is being investigated by additional control experiments to test whether free nickel oxide transforms into a non-reduced $NiAl_2O_4$ phase with multiple TPR/TPO cycles at various temperatures [33]. A competing cause is likely incomplete sulfur removal from the pilot-scale catalyst that results in the formation of surface and bulk nickel sulfide and sulfate species that are inactive for further reforming, and chemistry involved in sulfur removal during catalyst regeneration is being explored using X-ray absorption spectroscopy.

The post-reaction samples were also analyzed with SEM/EDS, shown in Figs. 4, 5. At a macroscopic, catalyst particle scale ($\sim$200 μm), there is no discernible difference among the samples, as the support is a relatively non-porous, attrition resistant material. Following use in both fluidized-bed reactors, however, some surface morphology differences were observed. The sample used in the fixed-bed reactor maintains a relatively rough surface with distinct nickel crystallites (represented by the light spots in Fig. 4b). The catalysts that were used in the bubbling fluidized bed and recirculating/regenerating reactors (Fig. 4d, f) show that the particle surface has been somewhat smoothed as a result of inter-particle collisions occurring within the reactor. EDS spectra for these samples (Fig. 5) show the expected components of the catalyst and support (Ni, Mg, K, Al, and Si). The sample used in the fixed-bed reactor had a higher nickel EDS signal than the catalysts used in the fluidized/circulating reactors in which surface abrasion may result in a small loss of surface nickel species. Alternatively, diffusion of nickel into the bulk of catalyst support would also result in a decrease in nickel intensity via EDS, which is consistent with the higher proportion of spinel nickel aluminate on the catalysts used in the fluidized/circulating reactors as compared to the catalyst tested in the fixed-bed reactor. The catalyst sample used in the recirculating/regenerating reactor (iii) did not show a clear potassium signal on EDS as its as-synthesized potassium content was only 10 % of catalyst (i) and (ii).

Taken together, these results indicate that nickel alumina catalysts used with raw syngas in cyclic operations are regenerable, though changes in the active nickel species and their extent of reducibility change with time on stream. The catalyst used with model syngas does not exhibit these changes. Additionally, the catalyst used with model syngas in recirculating/regenerating conditions showed that high levels of steady-state methane and tar conversion could be achieved, indicating that permanent catalyst deactivation can be avoided by limiting the catalyst to short periods of H_2S exposure before regeneration. Thus, some other non-H_2S component(s) including tars and inorganics present in biomass-derived syngas may contribute to and accelerate deactivation by poisoning and phase transformation. In this context, regeneration conditions based on bench-scale results should be studied and adapted for use in a pilot-scale, recirculating/regenerating reactor.

4 Conclusions

Fluidizable $NiMgK/Al_2O_3$ catalysts were tested for multiple reaction cycles at both bench- and pilot-scales, using real and simulated biomass-derived syngas. Multiple

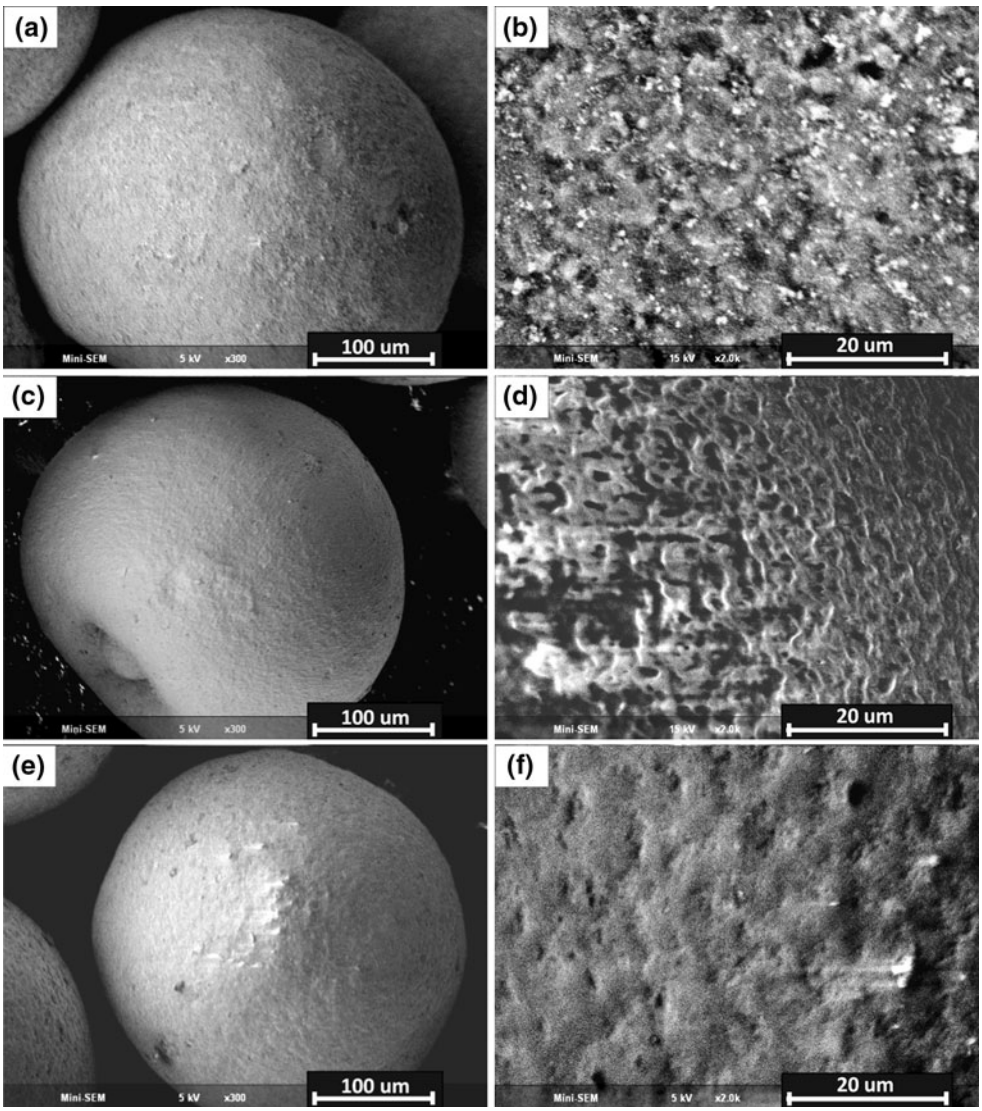

Fig. 4 SEM micrographs at ×300 and ×2,000 of post-reaction catalysts tested in (**a**, **b**) fixed-bed reactor, bench-scale conditions with model syngas, (**c**, **d**) pilot-plant fluidized bed reactor with real syngas, and (**e**, **f**) pilot-plant recirculating/regenerating reactor using model syngas

reactor configurations and conditions were employed, with the goal of demonstrating how these configurations affected methane and tar conversions over multiple catalyst regeneration cycles. The catalyst used at the pilot-scale with raw syngas lost activity between reaction cycles. The regeneration protocol, which successfully removed sulfur and restored activity on catalysts used with model syngas, was used on deactivated catalyst that had been exposed to raw syngas. This regeneration process involving steam oxidation and H_2 reduction restored activity to the spent catalyst, over multiple reaction cycles. Characterization by TPR suggests that the loss of reducible nickel, especially the NiO phase corresponding to the low-temperature nickel oxide reduction feature, is related to the decrease in catalyst activity, due to the formation of nickel aluminate. Finally, a recirculating/regenerating reactor was evaluated to decrease the extent of sulfur-poisoning before the catalyst was regenerated. This recirculating/regenerating reactor was able to achieve a high (>90 %) steady-state conversion of methane for >100 h or operation, indicating that this reaction/regeneration approach might be suitable for maintaining catalyst activity on an industrially-relevant time scale and number of reaction cycles, which was a successful demonstration of biomass-derived syngas catalytic conditioning. Additionally, the differences in catalyst performance using a simulated and real, biomass-derived syngas stream indicate that there are components present in the real stream that are not adequately modeled in the syngas stream. Heavy tars and polycyclic aromatics are known to be present in real syngas, and the use of benzene and naphthalene as surrogates may be insufficient. In addition, some inorganics found in biomass, which become

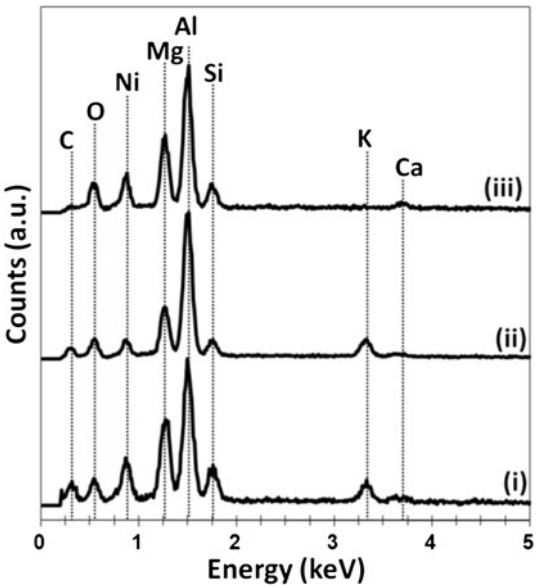

Fig. 5 Energy-dispersive spectroscopy spectra of post-reaction catalysts tested in (*i*) fixed-bed reactor, bench-scale conditions with model syngas ($NiMgK/Al_2O_3$), (*ii*) pilot-plant fluidized bed reactor with real syngas ($NiMgK/Al_2O_3$), and (*iii*) pilot-plant recirculating/regenerating reactor using model syngas ($NiMgK_{0.1}/Al_2O_3$)

concentrated in the ash following biomass gasification, may be transported to the reforming reactor where they can interact with catalysts. Therefore, in order to gain more representative results for how a catalyst were perform on an industrial, with real contaminants, appropriate small-scale biomass solids feeders or slip-streams of real process gas should be employed.

Acknowledgments The authors would like to thank the U. S. Department of Energy's Biomass Program contract DE-AC36-99-GO-10337 for funding this work and the industrial collaborator for evaluating the catalyst on the pilot-scale recirculating/regenerating reactor and for sharing the reaction results.

References

1. Milne TA, Abatzoglou N, Evans RJ (1998) Biomass gasification "tars": their nature, formation and conversion. NREL Technical Report, Golden, Report No. NREL/TP 570-25357
2. Dayton D (2002) A review of the literature of catalytic biomass tar destruction, NREL Technical Report, Golden, Report No. NREL/TP-510-32815
3. Devi L, Ptasinski KJ, Janssen FJJG (2003) Biomass Bioenergy 24:125
4. Yung MM, Jablonski WS, Magrini-Bair KA (2009) Energy Fuels 23:1874–1887
5. Bain RL, Dayton DC, Carpenter DL, Czernik SR, Feik CJ, French RJ, Magrini-Bair KA, Phillips SD (2005) Ind Eng Chem Res 44:7945
6. Phillips SD (2007) Ind Eng Chem Res 46:8887–8897
7. Vassilatos V, Taralas G, Sjiiskiim K, Bjombom E (1992) J Canadian Chem Eng 70:1008–1013
8. Devi L, Craje M, Thüne P, Ptasinski KJ, Janssen FJJG (2005) Appl Catal A Gen 294:68–79
9. Corella J, Toldeo JM, Padilla R (2004) Energy Fuels 18:713–720
10. Ammendola P, Lisi L, Piriou B, Ruoppolo G (2009) Chem Eng J 154:361–368
11. Huber GW, Iborra S, Corma A (2006) Chem Rev 106:4044–4098
12. Torres W, Pansare SS, Goodwin JG (2007) Catal Rev 49:407–456
13. Aznar MP, Corella J, Delgado J, Lahoz J (2003) Ind Eng Chem Res 32:1–10
14. Arauzo J, Radlein D, Piskorz J, Scott DS (1994) Energy Fuels 8:1192–1196
15. Magrini-Bair KA, Czernik S, French R, Parent YO, Chornet E, Dayton DC, Feik C, Bain R (2007) Appl Catal A Gen 318:199–206
16. Czernik S, French R, Magrini-Bair K, Chornet E (2004) Energy Fuels 18:1738–1743
17. Simell P, Kurkela E, Stahlberg P, Hepola J (1996) Catal Today 27:55–62
18. Corella J, Toledo JM, Padilla R (2004) Ind Eng Chem Res 43:2433–2445
19. Olsbye U, Moen O, Slagtern A, Dahl IM (2009) Appl Catal A Gen 228:289–303
20. Chen X, Honda K, Zhang ZG (2005) Appl Catal A Gen 279:263–271
21. Sehested J (2003) J Catal 217:417–426
22. Hepola J, Simell P (1997) Appl Catal B Environ 14:305–321
23. Ashrafi M, Pfeifer C, Proll T, Hofbauer H (2008) Energy Fuels 22:4190–4195
24. Hepola J, McCarty J, Krishman G, Wong V (1999) Appl Catal B Environ 20:191–203
25. Lombard C, Le Doze S, Marencak E, Marquaire P-M, LeNoc D, Bertrand G, Lapicque F (2006) Int J Hydrogen Energy 31:437
26. Bartholomew CH, Agrawal PK, Katzer JR (1982) Adv Catal 31:135–235
27. Oudghiri-Hassani H, Abatzoglou N, Rakass S, Rowntree N (2007) J Power Sources 171:811–817
28. Rostrup-Nielsen JR (1971) J Catal 21:171–178
29. Yung MM, Magrini-Bair KA, Parent YO, Carpenter DL, Feik CJ, Gaston KR, Pomeroy MD, Phillips SD (2010) Catal Lett 134:242–249
30. Tomishige K, Miyazawa T, Kimura T, Kinimori K, Koizumi N, Yamada M (2005) Appl Catal B Environ 60:299–307
31. Rostrup-Nielsen JR, Sehested J, Norskov JK (2002) Adv Catal 47:65–139
32. Lappas AA, Samolada MC, Iatridis DK, Voutetakis SS, Vasalos IA (2004) Fuel 81:2087–2095
33. Tirsoaga A, Visinescu D, Jurca B, Ianculescu A, Carp O (2011) J Nanopart Res 13:6397–6408
34. Guo J, Lou H, Zhao H, Chai D, Zheng X (2004) Appl Catal A Gen 273:75–82
35. Santos DCRM, Lisboa JS, Passos FB, Noronha FB (2004) Braz J Chem Eng 21:203–209